SIMULATION OF ALPHA MAGNET ELEMENTS IN DIPOLE-ONLY TRACKING CODES[*,†]

J.W. Lewellen[#] and F. Krawczyk, AOT-AE, LANL, Los Alamos, NM 87544 USA

Abstract

Alpha magnets [1] are useful in a variety of ion-beam and low-energy (< 5 MeV) electron-beam transport systems as both "switchyard" elements and as bunch compressors [2,3]. A unique feature of the alpha-magnet is its broad-band achromatic transport. Particles of different energies, injected at a specific location and angle, will exit at the same location and (symmetry-reflected) angle but with a different time-of-flight.

Despite the general usefulness of alpha magnets in low-energy beam transport and compression schemes, few simulation codes support them as native elements. The (arguably) most-commonly-used codes used for injector design, PARMELA [4], ASTRA [5] and GPT [6] (listed in order of their release) support tracking of space-charge-dominated beams through dipole magnets, but do not support alpha magnets. As a result, these codes are unable to directly model a useful and interesting beam transport device.

We present an approximate method for simulating an alpha magnet in a tracking code using dipole elements. As the simulation code **elegant** [7] supports alpha magnets as well as multiple dipole models, it is used to provide a basic check of the approximation and a means of estimating the induced errors.

INTRODUCTION

Alpha magnets refer to a general class of achromatic bending magnets [1]. They are so-named because a particle beam traversing a properly aligned alpha magnet follows a trajectory reminiscent of the Greek letter α as shown in Figure 1. While alpha magnets in general can have a field dependence $B_z \sim G\, x^n$, $n{\geq}1$, quadrupolar alpha magnets (n=1) are the most practical to construct. Unless explicitly stated otherwise, the rest of this paper refers only to quadrupolar alpha magnets.

Figure 1 illustrates the achromatic nature of the alpha magnet: over a ±20% energy spread, electrons injected at the proper angle exit at the same point and angle; the trajectories are self-similar but have different overall length, facilitating the alpha magnet's use as a bunch compressor or stretcher, depending upon the chirp of the incoming beam. All particles cross the midplane, or x=0, line three times: at injection, at their maximum depth Δy within the alpha magnet, and at exit.

Using Borland's notation [8], the included half-angle of the alpha magnet θ_α is 40.71°. The general scaling factor for particle trajectories in an alpha magnet is

$$\alpha^2 = 5.867 \cdot 10^{-4} \mathrm{cm}^{-2}\, \frac{g[\mathrm{G/cm}]}{\beta\gamma}\;, \tag{1}$$

where g is the magnetic field gradient in Gauss cm⁻¹, γ is the particle's Lorentz factor, β is the particle's normalized velocity, and the product $\beta\gamma$ is the normalized momentum. The total path length of the particle's trajectory is

$$s_\alpha = \frac{\Lambda_\alpha}{\alpha} = 191.655\ \mathrm{cm} \cdot \sqrt{\frac{\beta\gamma}{g[\mathrm{G/cm}]}}\,, \tag{2}$$

the maximum depth the particle reaches is

$$\Delta y = \frac{\Delta Q_1}{\alpha} = 75.0513\ \mathrm{cm} \cdot \sqrt{\frac{\beta\gamma}{g[\mathrm{G/cm}]}}\,, \tag{3}$$

and the trajectory width is

$$\Delta x = \frac{\Delta Q_2}{\alpha} = 49.212\ \mathrm{cm} \cdot \sqrt{\frac{\beta\gamma}{g[\mathrm{G/cm}]}}\,. \tag{4}$$

Λ_α=4.642, ΔQ_1 = 1.818 and ΔQ_2 = 1.192 are the normalized path length, path depth and path width, respectively, and along with θ_α are invariants for quadrupole-type alpha magnets.
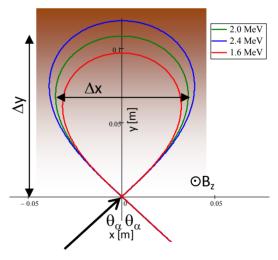

Figure 1: Three electron beam trajectories in an ideal quadrupolar alpha magnet: 2 MeV (green), 2.4 MeV (blue) and 1.6 MeV (red), all injected at the ideal injection angle along the line indicated by the black arrow. Background shading indicates relative magnetic field strength. The magnetic field gradient is 2.32 T/m.

The trajectory is self-similar for all choices of gradient and momentum, providing broadband achromaticity. For a fixed magnetic field gradient g and small variations of normalized momentum $\beta\gamma$ around a central value, the path

length varies approximately linearly with momentum, thus allowing the alpha magnet to be used as a chirper or stretcher; $R_{56} = s_\alpha/2 = \Lambda_\alpha/2\alpha$.

ALPHA MAGNET APPROXIMATION

Several approaches suggest themselves as means of implementing alpha magnets in accelerator tracking codes that do not natively support them, without needing to modify the source code.[*] For instance, one could export the beam distribution immediately before the alpha magnet, transform it by the transport matrix described in [8] via Matlab or another general-purpose numerical code, reimport it and continue with the simulation. However, this is awkward, generally non-portable and does not provide for including space-charge effects within the alpha magnet. One could also attempt to define an appropriate field map, but as the alpha magnet effectively redefines the z-axis for the beam, depending on the code this would also require exporting, processing and reimporting the beam distribution. Rather, one would prefer a method implementable completely within a single simulation code, and relatively easily translated from code to code.

An alpha magnet's magnetic field can be approximated by a series of N+1 dipoles with edges parallel to the x- (or the normalized-coordinate Q_2) axis, as illustrated in Figure 2. Since most beam dynamics code make at least some provision for modelling the effects of dipoles, this is our preferred method for emulating alpha magnets.
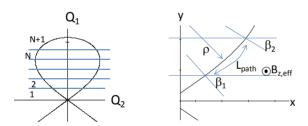

Figure 2: division of the alpha magnet into multiple dipole "slices (left), and a close-up of some important parameters for a given slice (right).

Our approach, in essence, breaks the alpha magnet up into N slices plus an (N+1)[th] "runout" or "turn-around" region encompassing the maximum, or midplane, depth reached by all particles in the beam.

To an extent, the number of slices, and thus slice width, is an arbitrary parameter. In a physical alpha magnet, particles entering with different energies will have differing maximum depths as they cross the midplane. In most beam dynamics codes, if a dipole is present in the beamline, every particle in the beam is constrained to enter it. Therefore, when approximating an alpha magnet with dipoles, the "deepest" slice must be arranged to

---

[*] One of GPT's unique features is the ability to add user-defined elements without risking corruption of its core algorithms (particle stepping, space-charge, etc.). Directly implementing an alpha magnet with GPT is thus relatively straightforward.

ensure that the lowest-energy particle in the beam would in fact reach it.

For each slice, and the (N+1)[th] "runout" region, the dipole parameters required by the specific beam-dynamics code (e.g. entrance / exit angles, magnetic field, bend radius, net bending angle, path length) are calculated via numerical integration of the normalized equations of motion through an ideal alpha magnet.

Once this exercise has been completed, so long as the number of slices does not change and certain other constraints are met, the edge angles remain constant and all other quantities scale with the α parameter, allowing for easy reuse of the model. Also, from symmetry, we need only calculate these parameters for one-half of the alpha magnet trajectory.

METHODOLOGY

Trajectory Calculation and Parameterization

A standalone numerical code, for instance MathCAD (used for this work), Matlab or Mathematica, is used to calculate the ideal trajectory of a particle from injection to the alpha magnet midplane using normalized coordinates as described in [8], allowing parameterization of the normalized transverse position (Q_2) and path length (L) as a function of normalized depth into the alpha magnet (Q_1). In turn, these permit us to define the angle θ of the particle's momentum vector with respect to the Q_1 (y) axis, as a function of depth. Figure 3 shows $Q_2(Q_1)$, $L(Q_1)$ and $\theta(Q_1)$ for the ideal trajectory from entrance point to maximum depth. Note that the horizontal axes on these plots corresponds to the vertical axis in Figure 2.
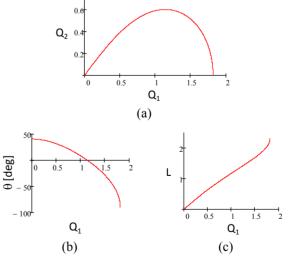

(a)

(b)

(c)

Figure 3: Normalized alpha magnet trajectory (a) transverse coordinate Q_2 vs. depth Q_1; (b) angle to the Q_1 axis vs. Q_1; (c) path length as a function of Q_1.

Dipole Slice Parameters

The magnetic field gradient g, the central momentum $\beta\gamma_o$, and the maximum depth Δy of the central trajectory within the alpha magnet are related by Equation 2; two

out of three of these parameters must be specified to compute the dipole slice parameters. The ratio of the minimum to the central momentum, $\beta\gamma_{min}/\beta\gamma_o$, is also required. Then the width of the slices in normalized coordinates along the Q_1 axis, is given by

$$w_{slice} = \frac{\Delta Q_1}{N} \cdot \sqrt{\eta \frac{\beta\gamma_{min}}{\beta\gamma_o}}, \qquad (5)$$

where η is a safety factor to allow for some variation in the injected beam momentum spread due to, for instance, optimization of upstream components.

Using N=8 slices, $\beta\gamma_{min}/\beta\gamma_o$=0.95, and η=0.9, w_{slice} = 0.21; the distance along the Q_1 axis between the start of the runout region and the depth of the central trajectory is $\Delta Q_1 - N w_{slice} = 0.138$. The slice width is therefore on the same order as the width of the runout region (assuming a symmetric momentum distribution), a condition we have empirically found works well.

Parameterization of the curves in Figure 3 yields the entrance and exit angles for each dipole slice (following the TRANSPORT [9] sign convention), and the normalized path length through each slice. These are presented in Table 1. Note that the "runout" slice is adjusted to transport the beam to the midplane of the alpha magnet.

Table 1: Slice Entry/Exit Angles and Path Lengths

Slice	From $Q_1=$	To $Q_1=$	β_1 [deg]	β_2 [deg]	$\delta\Lambda_\alpha$
1	0	0.210	40.71	-39.06	0.2749
2	0.210	0.420	39.06	-34.33	0.2630
3	0.420	0.630	34.33	-26.79	0.2450
4	0.630	0.840	26.79	-17.40	0.2275
5	0.840	1.051	17.40	-5.76	0.215
6	1.051	1.261	5.76	8.19	0.2107
7	1.261	1.471	-8.19	25.43	0.2201
8	1.471	1.681	-25.43	49.5	0.2657
runout	1.681	-	-49.5	0	0.3991

For an N-slice alpha magnet model, either 2N+1 or 2(N+1) dipoles must be defined, depending on whether one wishes to access the beam distribution at the midplane of the alpha magnet. Assuming the latter case, and using the nomenclature shown in Figure 4 as a reference, the following relationships exist between dipoles prior to and following the midplane:

- Dipoles on the same slice have the same magnetic field, bending radius and path length: $B_{n,e}=B_{n,i}$, $\rho_{n,e}=\rho_{n,i}$ and $L_{n,e}=L_{n,i}$ for n=1..N and runout.
- The dipole entrance and exit edge angles are related as: $\beta_{1,n+1,(i,e)} = -\beta_{2,n,(i,e)}$ for n=1..N and runout; $\beta_{2,R,i}=\beta_{1,R,e}=0$; and $\beta_{(2,1),n,e}=\beta_{(1,2),n,i}$ for n=1..N.

The magnetic field B_n for each slice is given by

$$B_n = \left(n - \frac{1}{2}\right) g \frac{w_{slice}}{\alpha}, \quad n \leq N \qquad (6)$$

Following the Nth slice, the field in the runout section is taken to be

$$B_R = \frac{\Delta Q_1}{\alpha} g, \qquad (7)$$

the nominal field at the central momentum trajectory midpoint. The physical path length and bending radius within each dipole slice is given by

$$L_n = \frac{\delta\Lambda\alpha}{\alpha} \text{ and }, \qquad (8)$$

and the bending radius of the central trajectory is

$$\rho_n = \frac{\beta\gamma_o m_e c}{q_e B_n} \qquad (9)$$

for all slices as well as the runout region.

The bend angle per slice can be set via two ways:

$$\theta_{FA,n} = \frac{L_n}{\rho_n}, \qquad (10a)$$

bases the bend angle per slice on the slice magnetic field and path length through the slice (the "field average" method), while

$$\theta_{EM,n} = \beta_{1,n} + \beta_{2,n}, n \leq N$$
$$\theta_{EM,R,i} = \beta_{1,n} + 90° \qquad (10b)$$
$$\theta_{EM,R,e} = \beta_{2,R} + 90°$$

bases the bend angle per slice on the edge angles, using the relationship that, for a rectangular bend magnet, the bend angle equals the sum of the edge angles. (The runout dipoles are special cases because their entrance and exit planes are perpendicular, not parallel.)
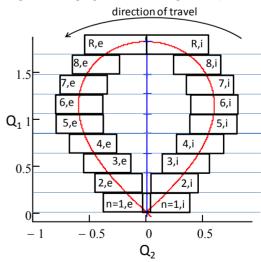

Figure 4: Dipole reference nomenclature; the beam passes through dipoles (n,i) before crossing the midplane, and dipoles (n,e) after passing the midplane.

ELEGANT TESTING

We use the beam dynamics code **elegant** to check the model: it has a built-in model for alpha magnets for reference; it has several dipole models and fine control over how they are implemented; and it can generate an R-matrix directly for a defined beamline.

For our test, we use a pencil electron beam with $\beta\gamma_o$=4.811 (2 MeV kinetic) and a $\pm$5% hard-edge momentum spread, and a magnetic field gradient g = 1 T/m, so α=11.04 m^{-1}. The other parameters are chosen to be consistent with the values given in Table 1, e.g. N=8 and η=0.9. Global default tracking was set to 2nd order, and both canonical sector bends (csbend element) and numerically integrated dipoles (nibend elements) were used to test the method.

Equations 11-13 show, respectively, the 1st-order transport matrices for **elegant**'s alpha magnet model (R_α), and csbend dipoles using edge-angle (R_{EM}) and field-average methods (R_{FA}) for calculating slice bend angles. Figure 5 and 6 plot x and x' vs $\beta\gamma$ at the exit of the alpha magnet for the test cases using csbend and nibend dipole models, respectively.

$$R_\alpha = \begin{pmatrix} -1 & -0.21 & 0 & 0 & 0 & 0 \\ 0 & -1 & 0 & 0 & 0 & 0 \\ 0 & 0 & -0.74 & 0.69 & 0 & 0 \\ 0 & 0 & -0.66 & -0.74 & 0 & 0 \\ 0 & 0 & 0 & 0 & 1 & 0.21 \\ 0 & 0 & 0 & 0 & 0 & 1 \end{pmatrix} \quad (11)$$

$$R_{EM} = \begin{pmatrix} -1 & -0.2 & 0 & 0 & 0 & 0 \\ 0 & -1 & 0 & 0 & 0 & 0.02 \\ 0 & 0 & -0.82 & 0.49 & 0 & 0 \\ 0 & 0 & -0.66 & -0.82 & 0 & 0 \\ 0 & 0.02 & 0 & 0 & 1 & 0.25 \\ 0 & 0 & 0 & 0 & 0 & 1 \end{pmatrix} \quad (12)$$

$$R_{FA} = \begin{pmatrix} -0.88 & -0.19 & 0 & 0 & 0 & 0.01 \\ 1.22 & -0.88 & 0 & 0 & 0 & -0.01 \\ 0 & 0 & -0.80 & 0.53 & 0 & 0 \\ 0 & 0 & -0.67 & -0.80 & 0 & 0 \\ -0.01 & 0.1 & 0 & 0 & 1 & 0.24 \\ 0 & 0 & 0 & 0 & 0 & 1 \end{pmatrix} \quad (13)$$
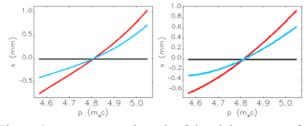

Figure 5: p-x space at the exit of the alpha magnet, for the built-in model (black), edge-angle method (red) and field-average method (blue) using **elegant**'s canonical sector bend (left) and numerically integrated bend (right) models.

CONCLUSIONS

A series of dipoles can be used to model the behavior of an alpha magnet in codes that do not natively include such elements. The "edge-angle" method for calculating dipole slice bend angle arguably provides somewhat more accurate first-order transport in the transverse planes, but the "field-average" method provides lower anomalous p-x coupling. Higher-order terms are more strongly dependent upon the details of the dipole model used.
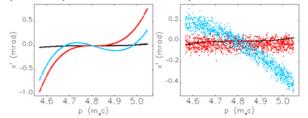

Figure 6: as in Figure 5, but plotting x' vs p.

This approach to approximating an alpha magnet was tested only using **elegant**. While the approach in general appears to be valid, the specifics of the dipole model a given beam dynamics code uses may have a significant impact upon the transverse dynamics, and in particular p-x and p-x' coupling. For instance, **elegant**'s numerically integrated dipole model, NIbend, produces notably different p-x' coupling than the canonical sector bend dipole model. Therefore, when using this approach with any beam dynamics code, we suggest at minimum determining the 1st-order transport matrix elements for comparison with **elegant**'s predictions for an equivalent momentum and trajectory depth.

REFERENCES

[1] H.A. Enge, "Achromatic Magnetic Mirror for Ion Beams," Rev. Sci. Instrum. **34**, p. 385 (1963). DOI: 10.1063/1.1718372

[2] S.V. Bensen et al., "The Stanford Mark III Infrared Free Electron Laser," Nucl. Instrum. Meth. A, vol 250, p. 39 (1986). DOI: 10.1016/0168-9002(86)90857-0

[3] J.W. Lewellen et al., "A Hot-Spare Injector for the APS Linac," Proc. 1999 Part. Accel Conf, New York, NY, p. 1979 (1999).

[4] J.H. Billen and L. Young. "Parmela User's Manual," LA-UR-96-1835 (1996).

[5] K. Floettmann, ASTRA User's Manual, 2000, http://www.desy.de/~mpyflo/Astra_dokumentation/

[6] M.J. de Loos and S.B van der Geer, "General Particle Tracer: a New 3D Code for Accelerator and Beam Line Design," Proc. 5th European Part. Accel. Conf., Sitges, Barcelona, p. 1241 (1996).

[7] M. Borland, "elegant: a Flexible SDDS-Compliant Code for Accelerator Simulation," Advanced Photon Source Light Source Note LS-287 (2000). DOI: 10.2172/761286

[8] M. Borland, "A High-Brightness Thermionic Microwave Electron Gun," Ph.D. thesis, Stanford University, 1991.

[9] D.C. Carey, K.L. Brown and F. Rothacker, "Third-Order TRANSPORT with MAD Input," SLAC-R-530, page 126 (1998).